Chapter 2

A robust adaptive numerical method for singularly perturbed degenerate parabolic convection-diffusion problems

In this chapter, we consider a singularly perturbed degenerate parabolic convection-diffusion problem with the perturbation parameter ε such that $0 \leq \varepsilon \ll 1$. Let the domain be $\bar{G} = G \cup \partial G$, where $G := G_x \times (0, T]$ with $G_x = (0, 1)$. Suppose $\partial G = \Gamma_b \cup \Gamma_r \cup \Gamma_l$ with $\Gamma_b = [0, 1] \times \{0\}$, $\Gamma_l = \{0\} \times (0, T]$, and $\Gamma_r = \{1\} \times (0, T]$. On this domain we define the model problem as follows

$$\begin{cases} \mathcal{L}y(x,t) := (\mathcal{L}_\varepsilon - \frac{\partial}{\partial t})y(x,t) = f(x,t), \quad (x,t) \in G, \\ y(x,0) = g_b(x), \ x \in \bar{G}_x, \\ y(0,t) = g_l(t), \ y(1,t) = g_r(t), \ t \in (0,T], \end{cases} \tag{2.1}$$

where

$$\begin{cases} \mathcal{L}_\varepsilon y(x,t) := \varepsilon \frac{\partial^2 y}{\partial x^2}(x,t) + a(x)\frac{\partial y}{\partial x}(x,t) - b(x,t)y(x,t), \\ a(x) = a_0(x)x^p, \ p \geq 1, \\ a_0(x)\big|_{\bar{G}_x} \geq \underline{a} > 0, \\ b(x,t)\big|_{\bar{G}} \geq \beta > 0. \end{cases}$$

The function f and the coefficients a_0 and b are assumed to be sufficiently smooth. Further, sufficient compatibility conditions at the corners are considered such that

problem (2.1) possesses a unique solution and it is sufficiently smooth [5]. The considered problem (2.1) is known as a boundary turning point problem, since at $x = 0$, the coefficient of the convection term satisfies $a(x) = 0$. The point $x = 0$ is called a simple turning point for $p = 1$, and a multiple turning point for $p > 1$. Such problems arise in the modelling of heat flow and mass transport near an oceanic rise [76]. In [110], degenerate PDEs are developed on a non-rectangular domain for convection-diffusion problems without a turning point. Some multiple turning point problems are given in [77] that arise in the modelling of thermal boundary layers in a laminar flow.

It is shown that $y = v + w$, where v and w satisfy [79, 80]

$$\left\| \frac{\partial^{s+r} v}{\partial x^s \partial t^r} \right\|_{\bar{G}} \leq C(1 + \varepsilon^{1-\frac{s}{2}}), \ 0 \leq s + 2r \leq 3, \tag{2.2}$$

and

$$\left| \frac{\partial^{s+r} w}{\partial x^s \partial t^r} \right| \leq C\varepsilon^{-s/2} e^{-\sqrt{\beta}x/\sqrt{\varepsilon}}, \ (x,t) \in \bar{G}, \ 0 \leq s + 2r \leq 3, \tag{2.3}$$

respectively.

The main objective of this chapter is to construct a parameter-robust adaptive numerical method for problem (2.1). Firstly, the problem is semidiscretized in time using the implicit Euler method to get the linear stationary differential equations in space variable. The first order parameter-robust convergence of the time semidiscretization is proved. Then, these differential equations are approximated using the standard upwind scheme on a non-uniform spatial mesh generated through the equidistribution principle. The monitor function we consider here is a combination of an appropriate power of second order derivative of the solution and a positive constant. We provide parameter-robust convergence analysis of the method based on the truncation error and barrier function approach. The method is shown to be

first order parameter-robust convergent in both space and time. At the end, the method is implemented on two test examples to validate the theory.

This chapter is organized as follows: In Section 2.1, we consider the semidiscretization of problem (2.1) in time and prove that it is first order parameter-robust convergent. In Section 2.2, the layer-adaptive spatial mesh is generated and the fully discrete scheme is given on this mesh. Section 2.3 is devoted to parameter-robust convergence of the fully discrete scheme. In Section 2.4, we present the numerical algorithm and consider two test examples for validation of the theory. Finally, conclusions are included in Section 2.5.

2.1 The time semidiscretization

We consider the implicit Euler scheme to discretize problem (2.1) on a uniform mesh with time step $\Delta t = \frac{T}{M}$, where M is taken to be the discretization parameter in the time direction. Thus, we define the temporal mesh $\{t_m = m\Delta t, m = 0, ..., M\}$. The continuous problem (2.1) in semidiscretized form can be written as

$$\begin{cases} y^0(x) = g_b(x), \ x \in \bar{G}_x, \\ \begin{cases} \text{For } m = 0, ..., M-1, \\ (\Delta t\mathcal{L}_\varepsilon - I)y^{m+1}(x) = -y^m(x) + \Delta t f(x, t_{m+1}), \ x \in G_x, \\ y^{m+1}(0) = g_l(t_{m+1}), \quad y^{m+1}(1) = g_r(t_{m+1}), \end{cases} \end{cases} \tag{2.4}$$

where I is the identity operator. We have the following minimum principle for the operator $(\Delta t\mathcal{L}_\varepsilon - I)$.

Lemma 2.1.1. [80] Consider the function $z^{m+1} \in C^2(\bar{G}_x)$ such that $z^{m+1}(0) \geq 0$, $z^{m+1}(1) \geq 0$, and $(\Delta t\mathcal{L}_\varepsilon - I)z^{m+1}(x)|_{G_x} \leq 0$. Then $z^{m+1}(x)|_{\bar{G}_x} \geq 0$.

The local truncation error involved in the time semidiscrete scheme (2.4) is given by $e_{m+1} = y(x, t_{m+1}) - \check{y}^{m+1}(x)$, where $\check{y}^{m+1}(x)$ solves the following problem

$$\begin{cases} (\Delta t \mathcal{L}_\varepsilon - I)\check{y}^{m+1}(x) = -y(x, t_m) + \Delta t f(x, t_{m+1}), \ x \in G_x, \\ \check{y}^{m+1}(0) = g_l(t_{m+1}), \quad \check{y}^{m+1}(1) = g_r(t_{m+1}). \end{cases} \tag{2.5}$$

Lemma 2.1.2. The time derivatives of y satisfy the following bound

$$\left\| \frac{\partial^s y}{\partial t^s} \right\|_{\bar{G}} \leq C, \quad 0 \leq s \leq 2.$$

Thus, the local error e_{m+1} satisfies

$$\|e_{m+1}\|_{\bar{G}_x} \leq C(\Delta t)^2,$$

and the global error satisfies

$$\sup_{m+1 \leq T/\Delta T} \|y(x, t_{m+1}) - y^{m+1}(x)\|_{\bar{G}_x} \leq C\Delta t.$$

Proof. The time derivatives are bounded by using the arguments in [78]. The bounds on local and global errors follow from the arguments in [111, 112]. □

The above lemma entails the first order parameter-robust convergence for the time semidiscretization process.

Lemma 2.1.3. Consider the decomposition of $\check{y}^{m+1}(x)$ as $\check{y}^{m+1}(x) = \check{v}^{m+1}(x) + \check{w}^{m+1}(x)$, where $\check{y}^{m+1}$, $\check{v}^{m+1}$, and $\check{w}^{m+1}$ satisfy

$$\left| \frac{\partial^s \check{y}^{m+1}(x)}{\partial x^s} \right| \leq C(1 + \varepsilon^{-s/2} e^{-\sqrt{\beta}x/\sqrt{\varepsilon}}),$$

$$\left| \frac{\partial^s \check{v}^{m+1}(x)}{\partial x^s} \right| \leq C(1 + \varepsilon^{1-\frac{s}{2}}),$$

$$\left|\frac{\partial^s \breve{w}^{m+1}(x)}{\partial x^s}\right| \leq C\varepsilon^{-s/2}e^{-\sqrt{\beta}x/\sqrt{\varepsilon}}, \quad 0 \leq s \leq 3, \text{ for all } x \in \bar{G}_x.$$

Proof. The proof follows using the arguments in [80]. □

2.2 Spatial mesh generation and discretization

2.2.1 Layer-adaptive equidistribution mesh

Here, we discuss the construction of a layer-adaptive mesh through equidistribution of a suitably chosen monitor function $\mathcal{M}(x, y(x, t_{m+1})) > 0$. A spatial mesh, $\bar{G}_x^{N,m+1} := \{0 = x_0^{m+1}, x_1^{m+1}, ..., x_N^{m+1} = 1\}$ is said to be equidistributed if

$$\int_{x_{i-1}^{m+1}}^{x_i^{m+1}} \mathcal{M}(z, y(z, t_{m+1}))dz = \frac{1}{N}\int_0^1 \mathcal{M}(z, y(z, t_{m+1}))dz, \quad 1 \leq i \leq N.$$

In other form, the equidistributed mesh can be seen as a mapping $x^{m+1} = x^{m+1}(\xi)$, which relates the computational coordinate $\xi \in [0, 1]$ to the physical coordinate $x^{m+1} \in [0, 1]$, defined by

$$\int_0^{x^{m+1}(\xi)} \mathcal{M}(z, y(z, t_{m+1}))dz = \xi\int_0^1 \mathcal{M}(z, y(z, t_{m+1}))dz. \tag{2.6}$$

Motivated from [55, 56, 58, 59, 113], we choose the monitor function given by

$$\mathcal{M}(x, y(x, t_{m+1})) = \alpha^{m+1} + \left|\frac{\partial^2 w}{\partial x^2}(x, t_{m+1})\right|^{1/2}. \tag{2.7}$$

Here, α^{m+1} is a positive constant introduced to maintain a reasonable division of mesh points throughout the spatial domain. The equidistribution of the monitor

function with $\alpha^{m+1} = 0$ results in mesh starvation outside the boundary layer regions. To approximate $\partial^2 w/\partial x^2$, we consider

$$\frac{\partial^2 w}{\partial x^2}(x, t_{m+1}) \approx \left(\frac{\eta}{\varepsilon}\right) e^{-\frac{\sqrt{\beta}x}{\sqrt{\varepsilon}}},$$

where η (independent of ε and x) is a constant. Hence

$$\int_0^1 \left|\frac{\partial^2 w}{\partial x^2}(x, t_{m+1})\right|^{1/2} dx \equiv \Lambda \approx 2|\eta|^{1/2}\beta^{-1/2}\left(1 - e^{-\frac{\sqrt{\beta}}{2\sqrt{\varepsilon}}}\right). \tag{2.8}$$

Now the equidistribution of (2.7) using definition (2.6) leads to the mapping

$$e^{\left(-\frac{\sqrt{\beta}}{2\sqrt{\varepsilon}}x^{m+1}(\xi)\right)} - \frac{\alpha^{m+1}}{\Lambda}x^{m+1}(\xi) = 1 - \left(\frac{\alpha^{m+1}}{\Lambda} + 1 - e^{(-\frac{\sqrt{\beta}}{2\sqrt{\varepsilon}})}\right)\xi. \tag{2.9}$$

A non-uniform mesh in physical coordinates $\{x_i^{m+1}\}_{i=1}^N$ corresponds to an equispaced mesh $\{\xi_i = i/N\}_{i=0}^N$ in computational coordinates. So, the above equation is written as

$$e^{\left(-\frac{\sqrt{\beta}}{2\sqrt{\varepsilon}}x_i^{m+1}\right)} - \frac{\alpha^{m+1}}{\Lambda}x_i^{m+1} = 1 - \left(\frac{\alpha^{m+1}}{\Lambda} + 1 - e^{(-\frac{\sqrt{\beta}}{2\sqrt{\varepsilon}})}\right)\frac{i}{N}. \tag{2.10}$$

Hence, the adaptively generated mesh points are given by the solution of the non-linear algebraic equation (2.10). Throughout the rest of the paper we take $\alpha^{m+1} = \Lambda$. Next, the following lemmas provide some important properties of the mesh structure.

Lemma 2.2.1. Suppose that the non-uniform mesh (2.10) is constructed by taking $\alpha^{m+1} = \Lambda$ and

$$\frac{2\sqrt{\varepsilon}}{\sqrt{\beta}} N \ln N < 1. \tag{2.11}$$

Then

$$x_{N/2-1} < \frac{2\sqrt{\varepsilon}}{\sqrt{\beta}} \ln N < x_{N/2}.$$

Proof. Putting $\alpha^{m+1} = \Lambda$ and $x_i^{m+1} = \frac{2\sqrt{\varepsilon}}{\sqrt{\beta}} \ln N$ into (2.10) and simplifying for i, we get

$$i = \frac{N - \left(1 - \frac{2\sqrt{\varepsilon}}{\sqrt{\beta}} N \ln N\right)}{2 - e^{-\frac{\sqrt{\beta}}{2\varepsilon}}}.$$

Now the proof immediately follows using the assumption (2.11). □

Lemma 2.2.2. For $i = 1, ..., N/2 - 1$, we have

$$h_i^{m+1} < \frac{6\sqrt{\varepsilon}}{\sqrt{\beta}(N - 2i)}.$$

Proof. The proof is based on the lower and upper bounds of x_i^{m+1} denoted by $\underline{x}_i^{m+1}$ and $\overline{x}_i^{m+1}$, respectively. From (2.10), we have

$$e^{\left(-\frac{\sqrt{\beta}}{2\sqrt{\varepsilon}} \overline{x}_i^{m+1}\right)} = 1 - \left(2 - e^{(-\frac{\sqrt{\beta}}{2\sqrt{\varepsilon}})}\right) \frac{i}{N}.$$

Hence

$$x_i^{m+1} < \overline{x}_i^{m+1} = -\frac{2\sqrt{\varepsilon}}{\sqrt{\beta}} \log\left(1 - S\frac{i}{N}\right), \tag{2.12}$$

where $S = \left(2 - e^{(-\frac{\sqrt{\beta}}{2\sqrt{\varepsilon}})}\right)$. Now we use the obtained upper bound in (2.10) to get

$$x_i^{m+1} > \underline{x}_i^{m+1} = -\frac{2\sqrt{\varepsilon}}{\sqrt{\beta}} \log\left(1 - S\frac{i}{N} - \frac{2\sqrt{\varepsilon}}{\sqrt{\beta}} \log\left(1 - S\frac{i}{N}\right)\right). \tag{2.13}$$

Thus, for $i = 1, ..., N/2 - 1$,

$$\begin{aligned} h_i^{m+1} < \overline{x}_i^{m+1} - \underline{x}_{i-1}^{m+1} &= \frac{2\sqrt{\varepsilon}}{\sqrt{\beta}} \log\left(1 + \frac{S + \frac{2\sqrt{\varepsilon}}{\sqrt{\beta}} N \log\left(\frac{N}{N - S(i-1)}\right)}{N - Si}\right) \\ &< \frac{2\sqrt{\varepsilon}}{\sqrt{\beta}} \log\left(1 + \frac{3}{N - 2i}\right) < \frac{6\sqrt{\varepsilon}}{\sqrt{\beta}(N - 2i)}. \end{aligned}$$

□

Lemma 2.2.3. For the mesh generated using (2.10), mesh-widths h_i^{m+1}, $i = 1, ..., N$, satisfy

$$h_i^{m+1} \leq CN^{-1}.$$

Proof. From (2.7), we have that $\Lambda = \alpha^{m+1} \leq \mathcal{M}(x, y(x, t_{m+1}))$. Now using the derivative bounds, we get

$$\int_0^1 \mathcal{M}(x, y(x, t_{m+1}))dx \leq C.$$

Thus, by the equidistribution principle, we get

$$\alpha^{m+1}h_i^{m+1} \leq \int_{x_{i-1}^{m+1}}^{x_i^{m+1}} \mathcal{M}(x, y(x, t_{m+1}))dx = \frac{1}{N}\int_0^1 \mathcal{M}(x, y(x, t_{m+1}))dx \leq CN^{-1}.$$

Hence, $h_i^{m+1} \leq CN^{-1}$. □

2.2.2 The fully discrete scheme

Here, we shall discretize problem (2.4) on a non-uniform spatial mesh $\bar{G}_x^{N,m} = \{0 = x_0^m < x_1^m < ... < x_N^m = 1\}$, where m represents the time level and the step sizes are defined by $h_i^m = x_i^m - x_{i-1}^m,\ 1 \leq i \leq N$. On this spatial mesh, for any mesh function u with $u(x_i, t_m) = u_i^m$, we consider the following difference operators

$$D_x^+ u_i^m = \frac{u_{i+1}^m - u_i^m}{h_{i+1}^m}, \qquad D_x^- u_i^m = \frac{u_i^m - u_{i-1}^m}{h_i^m}, \qquad \delta_x^2 u_i^m = \frac{D_x^+ u_i^m - D_x^- u_i^m}{(h_i^m + h_{i+1}^m)/2}.$$

We shall use the term $Y(x_i^{m+1}, t_m)$ in the discretization of (2.4) as it is found by the linear interpolation of $Y(x_i^m, t_m),\ 0 \leq i \leq N$. Now the fully discrete scheme is given

by

$$\begin{cases} Y_i^0 = g_b(x_i^1) \text{ for } 0 \le i \le N, \\ \begin{cases} \text{For } m = 0, ..., M-1, \\ (\Delta t L_\varepsilon^N - I) Y_i^{m+1} = -Y(x_i^{m+1}, t_m) + \Delta t f(x_i^{m+1}, t_{m+1}) \text{ for } 1 \le i \le N-1, \\ Y_0^{m+1} = g_l(t_{m+1}), \quad Y_N^{m+1} = g_r(t_{m+1}), \end{cases} \end{cases} \tag{2.14}$$

where the discrete operator L_ε^N is defined by

$$L_\varepsilon^N Y_i^{m+1} := \varepsilon \delta_x^2 Y_i^{m+1} + a_i D_x^+ Y_i^{m+1} - b_i^{m+1} Y_i^{m+1}.$$

After rearrangement of the terms we can rewrite the equation (2.14) as

$$\begin{aligned} s_i^{m+1,-} Y_{i-1}^{m+1} + s_i^{m+1,\star} Y_i^{m+1} + s_i^{m+1,+} Y_{i+1}^{m+1} = q_i^{m+1}, \ 1 \le i \le N-1, \\ Y_0^{m+1} = g_l(t_{m+1}), \quad Y_N^{m+1} = g_r(t_{m+1}), \end{aligned} \tag{2.15}$$

where the coefficients $s_i^{m+1,-}$, $s_i^{m+1,\star}$ and $s_i^{m+1,+}$ are given by

$$\begin{aligned} s_i^{m+1,-} &= \tfrac{2\varepsilon\Delta t}{h_i^{m+1}(h_i^{m+1}+h_{i+1}^{m+1})}, \qquad s_i^{m+1,+} = \tfrac{2\varepsilon\Delta t}{h_{i+1}^{m+1}(h_i^{m+1}+h_{i+1}^{m+1})} + \tfrac{\Delta t a(x_i^{m+1})}{h_{i+1}}, \\ s_i^{m+1,\star} &= -1 - \Delta t b(x_i^{m+1}, t_{m+1}) - s_i^{m+1,-} - s_i^{m+1,+}, \\ q_i^{m+1} &= -\widetilde{Y}(x_i^{m+1}, t_m) + \Delta t f(x_i^{m+1}, t_{m+1}), \end{aligned}$$

and $\widetilde{Y}$ denotes the piecewise-linear interpolant of Y. Suppose $\widetilde{V}$ denotes the piecewise-linear interpolant of V. Then v is approximated as follows

$$\begin{aligned} [\Delta t(a_i D_x^+ - b_i^{m+1}) - I] V_i^{m+1} = -\widetilde{V}(x_i^{m+1}, t_m) + \Delta t f(x_i^{m+1}, t_{m+1}), \quad 1 \le i \le N-1, \\ V_i^0 = g_b(x_i^1), i = 0, 1, \ldots, N, \quad V_N^{m+1} = g_r(t_{m+1}). \end{aligned} \tag{2.16}$$

2.3 Error analysis

We consider spatial discretization of problem (2.5) for error analysis. So, we consider the following difference equation

$$\begin{cases} (\Delta L_\varepsilon^N - I)\check{Y}_i^{m+1} = s_i^{m+1,-}\check{Y}_{i-1}^{m+1} + s_i^{m+1,\star}\check{Y}_i^{m+1} + s_i^{m+1,+}\check{Y}_{i+1}^{m+1} \\ \qquad\qquad\qquad\qquad = \check{q}_i^{m+1}, \ 1 \le i \le N-1, \\ \check{Y}_0^{m+1} = g_l(t_{m+1}), \quad \check{Y}_N^{m+1} = g_r(t_{m+1}), \end{cases} \tag{2.17}$$

where $s_i^{m+1,-}$, $s_i^{m+1,\star}$, $s_i^{m+1,+}$ are as defined in (2.15) and $\check{q}_i^{m+1} = -y(x_i^{m+1}, t_m) + \Delta t\ f(x_i^{m+1}, t_{m+1})$. The operator $(\Delta t L_\varepsilon^N - I)$ satisfies the following discrete comparison principle which can be proved using the standard arguments.

Lemma 2.3.1. (Discrete Comparison Principle) Suppose that the difference operator $(\Delta t L_\varepsilon^N - I)$ satisfies the following inequality

$$(\Delta t L_\varepsilon^N - I)P_i^{m+1} \le (\Delta t L_\varepsilon^N - I)Q_i^{m+1}, \quad 1 \le i \le N-1,$$

with $P_0^{m+1} \ge Q_0^{m+1}$ and $P_N^{m+1} \ge Q_N^{m+1}$, then $P_i^{m+1} \ge Q_i^{m+1}$ for $0 \le i \le N$.

We decompose $\check{Y}$ as follows

$$\check{Y}_i^{m+1} = \check{V}_i^{m+1} + \check{W}_i^{m+1},$$

where

$$\begin{cases} (\Delta t L_\varepsilon^N - I)\check{V}_i^{m+1} = -v(x_i^{m+1}, t_m) \\ \qquad\qquad\qquad + \Delta t f(x_i^{m+1}, t_{m+1}), \ 1 \le i \le N-1, \ 1 \le m \le M-1, \\ \check{V}_0^{m+1} = v(x_0^{m+1}, t_{m+1}), \ \check{V}_N^{m+1} = v(x_N^{m+1}, t_{m+1}), \end{cases} \tag{2.18}$$

and

$$\begin{cases} (\Delta t L_\varepsilon^N - I)\check{W}_i^{m+1} = -w(x_i^{m+1}, t_m), \quad 1 \le i \le N-1,\ 1 \le m \le M-1, \\ \check{W}_0^{m+1} = w(x_0^{m+1}, t_{m+1}),\ \check{W}_N^{m+1} = w(x_N^{m+1}, t_{m+1}). \end{cases} \tag{2.19}$$

We will bound errors in the smooth and singular components separately and combine them with the help of a triangle inequality as follows

$$|\check{Y}_i^{m+1} - \check{y}^{m+1}(x_i^{m+1})| \le |\check{V}_i^{m+1} - \check{v}^{m+1}(x_i^{m+1})| + |\check{W}_i^{m+1} - \check{w}^{m+1}(x_i^{m+1})|. \tag{2.20}$$

Next we consider the discrete Padé approximation of the function $e^{-\frac{\sqrt{\beta}x_i^{m+1}}{2\sqrt{\varepsilon}}}$ and prove some technical results to be used later.

Lemma 2.3.2. Consider a mesh function T_i^{m+1} such that

$$T_0^{m+1} = 1, \quad T_i^{m+1} = \prod_{l=1}^{i} \left(1 + \frac{\sqrt{\beta} h_l^{m+1}}{2\sqrt{\varepsilon}}\right)^{-1}, \quad i = 1, ..., N.$$

Then, for $i = 1, ..., N-1$, we have

$$(\Delta t L_\varepsilon^N - I)T_i^{m+1} \le -\frac{C\Delta t}{2\sqrt{\varepsilon}/\sqrt{\beta} + h_{i+1}^{m+1}} T_i^{m+1}.$$

Proof. We have

$$\frac{T_i^{m+1} - T_{i-1}^{m+1}}{h_i} = -\frac{\sqrt{\beta}}{2\sqrt{\varepsilon}} T_i^{m+1}.$$

Applying the discrete operator $(\Delta t L_\varepsilon^N - I)$ to T_i^{m+1}, we get

$$\begin{aligned} (\Delta t L_\varepsilon^N - I)T_i^{m+1} &= \Delta t \left[\varepsilon \delta_x^2 T_i^{m+1} + a_i D_x^+ T_i^{m+1} - b_i^{m+1} T_i^{m+1}\right] - T_i^{m+1} \\ &= \Delta t \left\{ \frac{2\varepsilon}{h_i^{m+1} + h_{i+1}^{m+1}} \left[-\frac{\sqrt{\beta}}{2\sqrt{\varepsilon}} T_{i+1}^{m+1} + \frac{\sqrt{\beta}}{2\sqrt{\varepsilon}} T_{i+1}^{m+1} \left(1 + \frac{\sqrt{\beta} h_{i+1}^{m+1}}{2\sqrt{\varepsilon}}\right)\right]\right. \end{aligned}$$

$$
\begin{aligned}
&\qquad + a_i\left(\frac{-\sqrt{\beta}}{2\sqrt{\varepsilon}}\right)T_{i+1}^{m+1} - b_i^{m+1}T_i^{m+1}\Big\} - T_i^{m+1}\\
&\leq \frac{-\sqrt{\beta}\Delta t}{2\sqrt{\varepsilon}+\sqrt{\beta}h_{i+1}^{m+1}}\Bigg[a_i - \frac{\sqrt{\varepsilon}\sqrt{\beta}h_{i+1}^{m+1}}{h_i^{m+1}+h_{i+1}^{m+1}}\\
&\qquad + \frac{b_i^{m+1}(2\sqrt{\varepsilon}+\sqrt{\beta}h_{i+1}^{m+1})}{\sqrt{\beta}}\Bigg]T_i^{m+1}\\
&\leq -\frac{\Delta t}{2\sqrt{\varepsilon}/\sqrt{\beta}+h_{i+1}^{m+1}}\left[a_i + \frac{\sqrt{\varepsilon}}{\sqrt{\beta}}(2b_i^{m+1}-\beta) + b_i^{m+1}h_{i+1}^{m+1}\right]T_i^{m+1}\\
&\leq -\frac{C\Delta t}{2\sqrt{\varepsilon}/\sqrt{\beta}+h_{i+1}^{m+1}}T_i^{m+1}.
\end{aligned}
$$

□

Lemma 2.3.3. The mesh function T_i^{m+1} satisfies

$$e^{-\frac{\sqrt{\beta}x_i^{m+1}}{2\sqrt{\varepsilon}}} \leq T_i^{m+1}, \quad i = 1, ..., N. \tag{2.21}$$

Also,

$$T_{N/2-1}^{m+1} \leq CN^{-1}.$$

Proof. We know that, for any positive real number p, $e^{-p} < 1/(1+p)$; so working for each i, we can easily get that

$$e^{-\frac{\sqrt{\beta}x_i^{m+1}}{2\sqrt{\varepsilon}}} = \prod_{l=1}^{i} e^{-\frac{\sqrt{\beta}h_l^{m+1}}{2\sqrt{\varepsilon}}} \leq \prod_{l=1}^{i}\left(1+\frac{\sqrt{\beta}h_l^{m+1}}{2\sqrt{\varepsilon}}\right)^{-1} = T_i^{m+1}.$$

This proves (2.21). Now using the bound on mesh size from Lemma 2.2.2, we have

$$
\begin{aligned}
\log\left(\prod_{l=1}^{N/2-1}\left(1+\frac{\sqrt{\beta}h_l^{m+1}}{2\sqrt{\varepsilon}}\right)\right) &= \sum_{l=1}^{N/2-1}\log\left(1+\frac{\sqrt{\beta}h_l^{m+1}}{2\sqrt{\varepsilon}}\right)\\
&> \sum_{l=1}^{N/2-1}\left(\frac{\sqrt{\beta}h_l^{m+1}}{2\sqrt{\varepsilon}} - \frac{1}{2}\left(\frac{\sqrt{\beta}h_l^{m+1}}{2\sqrt{\varepsilon}}\right)^2\right)\\
&> \frac{\sqrt{\beta}x_{N/2-1}^{m+1}}{2\sqrt{\varepsilon}} - \frac{9}{8}\sum_{l=1}^{N/2-1}\frac{1}{l^2} > \frac{\sqrt{\beta}x_{N/2-1}^{m+1}}{2\sqrt{\varepsilon}} - \frac{9}{4}.
\end{aligned}
$$

Thus

$$\prod_{l=1}^{N/2-1}\left(1+\frac{\sqrt{\beta}h_l^{m+1}}{2\sqrt{\varepsilon}}\right)^{-1} < e^{\frac{9}{4}-\frac{\sqrt{\beta}x_{N/2-1}^{m+1}}{2\sqrt{\varepsilon}}} < Ce^{-\frac{\sqrt{\beta}x_{N/2-1}^{m+1}}{2\sqrt{\varepsilon}}}.$$

Now from the mapping (2.10), we have

$$e^{-\frac{\sqrt{\beta}x_{N/2-1}^{m+1}}{2\sqrt{\varepsilon}}} = x_{N/2-1}^{m+1}+1-\frac{N-2}{2N}(2-e^{-\frac{\sqrt{\beta}}{2\sqrt{\varepsilon}}}) < x_{N/2-1}^{m+1}+2N^{-1} < \frac{2\sqrt{\varepsilon}}{\sqrt{\beta}}\log N+2N^{-1}.$$

So, using assumption (2.11), we obtain

$$T_{N/2-1}^{m+1} \leq CN^{-1}.$$

□

2.3.1 Error analysis of the regular component

Lemma 2.3.4. For $i=0,...,N$, the error in the regular component $\check{V}_i^{m+1}$ satisfies

$$|\check{V}_i^{m+1}-\check{v}^{m+1}(x_i^{m+1})| \leq CN^{-1}.$$

Proof. The local truncation error at time level $m+1$ is given by

$$\begin{aligned}
\eta_i^{m+1}(\check{V}) &= (\Delta t L_\varepsilon^N - I)(\check{V}_i^{m+1}-\check{v}^{m+1}(x_i^{m+1})) \\
&= \frac{\varepsilon\Delta t}{(h_i^{m+1}+h_{i+1}^{m+1})}\left[\frac{1}{h_{i+1}^{m+1}}\int_{x_i^{m+1}}^{x_{i+1}^{m+1}}(z-x_{i+1}^{m+1})^2\check{v}_{xxx}^{m+1}(z)dz\right. \\
&\quad \left.-\frac{1}{h_i^{m+1}}\int_{x_{i-1}^{m+1}}^{x_i^{m+1}}(z-x_{i-1}^{m+1})^2\check{v}_{xxx}^{m+1}(z)dz\right] \\
&\quad +\frac{\Delta t\ a(x_i^{m+1})}{h_i^{m+1}}\int_{x_{i-1}^{m+1}}^{x_i^{m+1}}(z-x_{i+1}^{m+1})\check{v}_{xx}^{m+1}(z)dz.
\end{aligned}$$

Thus

$$|\eta_i^{m+1}(\check{V})| \leq \varepsilon \Delta t \int_{x_{i-1}^{m+1}}^{x_{i+1}^{m+1}} |\check{v}_{xxx}^{m+1}(z)|dz + a_{\max} \Delta t \int_{x_{i-1}^{m+1}}^{x_i^{m+1}} |\check{v}_{xx}^{m+1}(z)|dz$$

where $a_{\max}$ is the maximum value of $a(x)$. Now using the derivative bounds (Lemma 2.1.3) and mesh sizes bound (from Lemma 2.2.3), we get

$$|\eta_i^{m+1}(\check{V})| \leq CN^{-1}. \tag{2.22}$$

Now applying the operator $(\Delta t L_\varepsilon^N - I)$ to the barrier function, $\Phi_i^\pm = CN^{-1} \pm (\check{V}_i^{m+1} - \check{v}^{m+1}(x_i^{m+1}))$, so that for $i = 1, ..., N-1$, we get

$$(\Delta t L_\varepsilon^N - I)\Phi_i^\pm = -(\Delta t b_i^{m+1} + 1)CN^{-1} \pm (\Delta t L_\varepsilon^N - I)(\check{V}_i^{m+1} - \check{v}^{m+1}(x_i^{m+1})) \leq 0,$$

with $\Phi_0^\pm \geq 0$ and $\Phi_N^\pm \geq 0$. Thus, using the discrete comparison principle, we get

$$|\check{V}_i^{m+1} - \check{v}^{m+1}(x_i^{m+1})| \leq CN^{-1}, \ i = 0, ..., N.$$

□

2.3.2 Error analysis of the singular component

Lemma 2.3.5. For $i = N/2 - 1, ..., N$, it holds

$$|\check{W}_i^{m+1} - \check{w}^{m+1}(x_i^{m+1})| \leq CN^{-1}.$$

Proof. We use (2.19) and (2.3) to get

$$|\check{W}_N^{m+1}| \leq Ce^{-\frac{\sqrt{\beta}}{\sqrt{\varepsilon}}} \leq Ce^{-\frac{\sqrt{\beta}}{2\sqrt{\varepsilon}}} = C\prod_{l=1}^{N} e^{-\frac{\sqrt{\beta}h_l^{m+1}}{2\sqrt{\varepsilon}}}.$$

Then using the arguments of Lemma 2.3.3, we get $|\check{W}_N^{m+1}| \leq CT_N^{m+1}$. Also, from (2.19), we get $|\check{W}_0^{m+1}| \leq C \leq CT_0^{m+1}$. Now

$$|(\Delta t L_\varepsilon^N - I)\check{W}_i^{m+1}| = |w(x_i^{m+1}, t_m)| \leq Ce^{-\frac{\sqrt{\beta}x_i^{m+1}}{\sqrt{\varepsilon}}} \leq Ce^{-\frac{\sqrt{\beta}x_i^{m+1}}{2\sqrt{\varepsilon}}} \leq CT_i^{m+1},$$

where we have used (2.3) and Lemma 2.3.3. It is easy to verify that $(\Delta t L_\varepsilon^N - I)T_i^{m+1} \leq -T_i^{m+1}$. Hence, an application of the discrete comparison principle with $\Psi_i^{\pm} = CT_i^{m+1} \pm \check{W}_i^{m+1}$ gives

$$|\check{W}_i^{m+1}| \leq CT_i^{m+1}, \quad \text{for } i = 0, ..., N. \tag{2.23}$$

From Lemma 2.3.3, we have that $T_{N/2-1}^{m+1} \leq CN^{-1}$. Since, T_i^{m+1} decreases as i increases, so for $i = N/2 - 1, ..., N$, we have

$$T_i^{m+1} \leq CN^{-1}. \tag{2.24}$$

Combining (2.23) and (2.24), we get

$$|\check{W}_i^{m+1}| \leq CN^{-1}. \tag{2.25}$$

From Lemma 2.1.3, for $i = N/2 - 1, ..., N$,

$$|\check{w}^{m+1}(x_i^{m+1})| \leq Ce^{-\frac{\sqrt{\beta}x_i^{m+1}}{\sqrt{\varepsilon}}} \leq Ce^{-\frac{\sqrt{\beta}x_i^{m+1}}{2\sqrt{\varepsilon}}} \leq Ce^{-\frac{\sqrt{\beta}x_{N/2-1}^{m+1}}{2\sqrt{\varepsilon}}} < CN^{-1}, \tag{2.26}$$

where we have used the fact from the proof of Lemma 2.3.3.

Thus, for the region outside the boundary layer, we obtain the desired result using equations (2.25) and (2.26) in the following triangle inequality

$$|\check{W}_i^{m+1} - \check{w}^{m+1}(x_i^{m+1})| \leq |\check{W}_i^{m+1}| + |\check{w}^{m+1}(x_i^{m+1})|.$$

□

Lemma 2.3.6. For $i = 1, ..., N/2 - 2$, we have

$$|\check{W}_i^{m+1} - \check{w}^{m+1}(x_i^{m+1})| \leq CN^{-1}.$$

Proof. Using Taylor expansions and the derivative bounds of $\check{w}^{m+1}$ from Lemma 2.1.3, we get

$$\begin{aligned} |\eta_i^{m+1}(\check{W})| &\leq \frac{C\Delta t}{\varepsilon}\int_{x_{i-1}^{m+1}}^{x_{i+1}^{m+1}} e^{-\frac{\sqrt{\beta}z}{\sqrt{\varepsilon}}}dz \leq \frac{C\Delta t}{\varepsilon}\int_{\xi_{i-1}}^{\xi_{i+1}} \frac{\Lambda e^{-\frac{\sqrt{\beta}x(\xi)}{\sqrt{\varepsilon}}}}{\alpha^{m+1} + |\check{w}_{xx}^{m+1}|^{1/2}}d\xi \\ &\leq \frac{C\Delta t}{\sqrt{\varepsilon}}\int_{\xi_{i-1}}^{\xi_{i+1}} e^{-\frac{\sqrt{\beta}x(\xi)}{2\sqrt{\varepsilon}}}d\xi < \frac{C\Delta t}{\sqrt{\varepsilon}N}e^{-\frac{\sqrt{\beta}x_{i-1}^{m+1}}{2\sqrt{\varepsilon}}} = \frac{C\Delta t}{\sqrt{\varepsilon}N}e^{-\frac{\sqrt{\beta}x_i^{m+1}}{2\sqrt{\varepsilon}}}e^{\frac{\sqrt{\beta}h_i^{m+1}}{2\sqrt{\varepsilon}}}. \end{aligned}$$

Also, from Lemma 2.2.2 we have $h_i^{m+1} < \frac{2\sqrt{\varepsilon}}{\sqrt{\beta}}\log\left(1 + \frac{3}{N-2i}\right)$. Thus, we get

$$|\eta_i^{m+1}(\check{W})| \leq \frac{C\Delta t}{\sqrt{\varepsilon}N}e^{-\frac{\sqrt{\beta}x_i^{m+1}}{2\sqrt{\varepsilon}}}.$$

Again, using Lemma 2.3.3, we get

$$|\eta_i^{m+1}(\check{W})| \leq \frac{C\Delta t}{\sqrt{\varepsilon}N}T_i^{m+1}.$$

Now we shall apply the discrete comparison principle to obtain an error bound for $\check{W}$. Consider $\psi_i^{m+1} = \frac{C}{N}(1 + T_i^{m+1})$, $i = 0, ..., N/2 - 1$. Then, using Lemmas 2.2.2

and 2.3.2, for $i = 1, ..., N/2 - 2$, we have

$$\begin{aligned}(\Delta t L_\varepsilon^N - I)(\check{W}_i^{m+1} - \check{w}^{m+1}(x_i^{m+1})) &= \eta_i^{m+1}(\check{W}) \geq -\frac{C\Delta t}{\sqrt{\varepsilon}N} T_i^{m+1} \\ &\geq \frac{C}{N}(\Delta t L_\varepsilon^N - I) T_i^{m+1} \\ &\geq (\Delta t L_\varepsilon^N - I)\psi_i^{m+1}.\end{aligned}$$

Also,

$$(\check{W}_0^{m+1} - \check{w}^{m+1}(x_0^{m+1})) \leq \psi_0^{m+1} \quad \text{and} \quad (\check{W}_{N/2-1}^{m+1} - \check{w}^{m+1}(x_{N/2-1}^{m+1})) \leq \psi_{N/2-1}^{m+1}.$$

Hence, using the discrete comparison principle, we have

$$(\check{W}_i^{m+1} - \check{w}^{m+1}(x_i^{m+1})) \leq \psi_i^{m+1}, \ i = 0, ..., N/2 - 1,$$

which implies that

$$(\check{W}_i^{m+1} - \check{w}^{m+1}(x_i^{m+1})) \leq CN^{-1}, \ i = 1, ..., N/2 - 2.$$

Now we repeat the above argument for $-(\check{W}_i^{m+1} - \check{w}^{m+1}(x_i^{m+1}))$. Thus, we have

$$|\check{W}_i^{m+1} - \check{w}^{m+1}(x_i^{m+1})| \leq CN^{-1}, \ i = 1, ..., N/2 - 2.$$

□

Theorem 2.3.1. Suppose $\check{y}^{m+1}(x_i^{m+1})$ and $\check{Y}_i^{m+1}$, respectively, are the solutions of (2.4) and (2.17). Then on the equidistributed mesh (2.10), we have

$$|\check{Y}_i^{m+1} - \check{y}^{m+1}(x_i^{m+1})| \leq CN^{-1}, \quad i = 0, ..., N.$$

Proof. The result follows by using Lemmas 2.3.4, 2.3.5, and 2.3.6 in inequality (2.20).

□

Corollary 2.3.1. If for some $0 < \sigma < 1$, $N^{-\sigma} \leq C\Delta t$, then from the previous theorem we have

$$|\check{Y}_i^{m+1} - \check{y}^{m+1}(x_i^{m+1})| \leq C\Delta t N^{-1+\sigma}, \quad i = 0, ..., N.$$

The constant σ in the above corollary does not influence numerical results given in the next section, and is used only for the theory. Such an assumption is common in the literature (see, e.g. [111, 114]). In the following theorem, we prove parameter-robust convergence of the fully discrete scheme. The analysis in this theorem is inspired from the works in [111, 114].

Theorem 2.3.2. Suppose y is the solution of (2.1) and $\{Y_i^{m+1}\}$ is the solution of the fully discrete scheme (2.14) at the $(m+1)$th time level. If for some $0 < \sigma < 1$, $N^{-\sigma} \leq C\Delta t$, then on each time level t_{m+1} we have

$$\|Y_i^{m+1} - y(x_i^{m+1}, t_{m+1})\|_{\bar{G}_x^{N,m+1}} \leq C(N^{-1+\alpha} + M^{-1}), \quad i = 0, ..., N.$$

Proof. We define the error of the fully discrete scheme at time level t_{m+1} by $E_i^{m+1} = Y_i^{m+1} - y(x_i^{m+1}, t_{m+1}), 0 \leq i \leq N$. We can split the global error as follows

$$\|E_i^{m+1}\|_{\bar{G}_x^{N,m+1}} \leq \|Y_i^{m+1} - \check{Y}_i^{m+1}\|_{\bar{G}_x^{N,m+1}} + \|\check{Y}_i^{m+1} - \check{y}^{m+1}(x_i^{m+1})\|_{\bar{G}_x^{N,m+1}} + \|\check{y}^{m+1}(x_i^{m+1}) - y(x_i^{m+1}, t_{m+1})\|_{\bar{G}_x^{N,m+1}}.$$

Using the results from Lemma 2.1.2 and Corollary 2.3.1, we obtain

$$\|E^{m+1}\|_{\bar{G}_x^{N,m+1}} \leq \|Y_i^{m+1} - \check{Y}_i^{m+1}\|_{\bar{G}_x^{N,m+1}} + C\Delta t(\Delta t + N^{-1+\sigma}). \tag{2.27}$$

Now considering (2.14), (2.17), and the stability of $(\Delta t L_\varepsilon^N - I)$, we get

$$\|Y_i^{m+1} - \check{Y}_i^{m+1}\|_{\bar{G}_x^{N,m+1}} \leq \|\widetilde{Y}(x_i^{m+1}, t_m) - y(x_i^{m+1}, t_m)\|_{\bar{G}_x^{N,m+1}}.$$

Then using a triangle inequality we get

$$\begin{aligned}\|\widetilde{Y}(x_i^{m+1}, t_m) - y(x_i^{m+1}, t_m)\|_{\bar{G}_x^{N,m+1}} \leq \|\widetilde{Y}(x_i^{m+1}, t_m) - \tilde{y}(x_i^{m+1}, t_m)\|_{\bar{G}_x^{N,m+1}} \\ + \|\tilde{y}(x_i^{m+1}, t_m) - y(x_i^{m+1}, t_m)\|_{\bar{G}_x^{N,m+1}}. \quad (2.28)\end{aligned}$$

The second term on right hand side of (2.28) is the interpolation error. Using standard arguments we get $\|\tilde{y}(x_i^{m+1}, t_m) - y(x_i^{m+1}, t_m)\|_{\bar{G}_x^{N,m+1}} \leq CN^{-1}$, and hence

$$\|\tilde{y}(x_i^{m+1}, t_m) - y(x_i^{m+1}, t_m)\|_{\bar{G}_x^{N,m+1}} \leq C\Delta t N^{-1+\sigma},$$

for some $0 < \sigma < 1$ such that $N^{-\sigma} \leq C\Delta t$.

The first term on right hand side of (2.28) is bounded using the stability of the interpolation operator. So, we get

$$\|\widetilde{Y}(x_i^{m+1}, t_m) - \tilde{y}(x_i^{m+1}, t_m)\|_{\bar{G}_x^{N,m+1}} \leq \|Y_i^m - y(x_i^m, t_m)\|_{\bar{G}_x^{N,m}}.$$

Thus

$$\|E^{m+1}\|_{\bar{G}_x^{N,m+1}} \leq \|E^m\|_{\bar{G}_x^{N,m}} + C\Delta t(\Delta t + N^{-1+\sigma}).$$

Hence, using a recursive argument, we obtain

$$\|E^{m+1}\|_{\bar{G}_x^{N,m+1}} \leq C(\Delta t + N^{-1+\sigma}).$$

□

2.4 Numerical experiments

We present numerical results for two test examples to validate the theory. To generate adaptive meshes we consider a moving mesh algorithm originally due to de Boor [47]. Starting with a uniform mesh the algorithm aims to construct a mesh that solves the following discrete equidistribution principle

$$h_i^m \mathcal{M}_i^m = \frac{1}{N} \sum_{j=1}^{N} h_j^m \mathcal{M}_j^m, \quad 1 \le i \le N, \tag{2.29}$$

where $\mathcal{M}_i^m$ is the discretized monitor function corresponding to (2.7). Kopteva and Stynes [71] remarked that the discrete equidistribution principle does not have to been enforced strictly, but it suffices to have

$$h_i^m \mathcal{M}_i^m \le \frac{\varrho}{N} \sum_{j=1}^{N} h_j^m \mathcal{M}_j^m, \quad 1 \le i \le N, \tag{2.30}$$

with a user-chosen constant $\varrho > 1$.

We note that the moving mesh algorithm considered here has been utilized for several classes of singularly perturbed problems in the literature (see [54, 58, 59, 71, 113, 115] and the references therein). However, there are only a few attempts to analyse its convergence. The algorithm is analysed in [72] for a stationary semilinear reaction-diffusion problem, in [71] for a stationary quasilinear convection-diffusion problem, and in [116] for regular boundary value problems. Algorithm 1 is used to generate the adaptive mesh and the solution at each time level.

Throughout the section we take $T = 1$, $M = N$ and the stopping constant $\varrho = 1.05$ for all numerical experiments.

Algorithm 1: Algorithm for the adaptive mesh and adaptive solution

Input: $N,\ M \in \mathbb{N},\ 0 < \varepsilon \leq 1$ and $\varrho > 1$.

Output: Adaptive mesh $\{x_i^k\}$ and adaptive solution Y_i^m at each time level t_m.

1. Choose a stopping constant $\varrho > 1$. Initialize the mesh iteration $\{x_i^{m,(k)}\}$ with $k = 0$ as the uniform mesh for $m = 1$, otherwise x_i^{m-1} for mth time level.

2. Solve the discrete problem (2.14) for $Y_i^{m,(k)}$ and (2.16) for smooth component $V_i^{m,(k)}$ on the spatial mesh $\{x_i^{m,(k)}\}$.

3. Compute the singular component as $W_i^{m,(k)} = Y_i^{m,(k)} - V_i^{m,(k)}$.

4. Construct the discretized monitor function by

$$\mathcal{M}_i^{m,(k)} = \alpha^{m,(k)} + |\delta_x^2 W_i^{m,(k)}|^{1/2}, \quad \text{for } i = 1, ..., N-1,$$

where $\alpha^{m,(k)}$ is defined by

$$\alpha^{m,(k)} = h_1^{m,(k)} |\delta_x^2 W_1^{m,(k)}|^{1/2} + \sum_{i=2}^{N-1} h_i^{m,(k)} \left\{ \frac{|\delta_x^2 W_{i-1}^{m,(k)}|^{1/2} + |\delta_x^2 W_i^{m,(k)}|^{1/2}}{2} \right\} + h_N^{m,(k)} |\delta_x^2 W_{N-1}^{m,(k)}|^{1/2}.$$

5. Set $H_i^{m,(k)} = h_i^{m,(k)} \left(\frac{\mathcal{M}_{i-1}^{m,(k)} + \mathcal{M}_i^{m,(k)}}{2} \right)$ for $i = 1, ..., N$, take $\mathcal{M}_0^{m,(k)} = \mathcal{M}_1^{m,(k)}$ and $\mathcal{M}_N^{m,(k)} = \mathcal{M}_{N-1}^{m,(k)}$. Then define $L_i^{m,(k)}$ by $L_i^{m,(k)} = \sum_{j=1}^{i} H_j^{m,(k)}$ for $i = 1, ..., N$ and $L_0^{m,(k)} = 0$.

6. **Stopping criteria**: Define $\varrho^{(k)}$ by $\varrho^{(k)} = \frac{N}{L_N^{m,(k)}} \max\limits_{i=1,...,N} H_i^{m,(k)}$. If $\varrho^{(k)} \leq \varrho$ then go to Step 8, else continue with Step 7.

7. Set $Z_i^{m,(k)} = i \frac{L_N^{m,(k)}}{N}$ for $i = 0, 1, ..., N$. Interpolate the points $(L_i^{m,(k)}, x_i^{m,(k)})$. Generate a new mesh $\{x_i^{m,(k+1)}\}$ by evaluating this interpolant at $Z_i^{m,(k)}$ for $i = 0, 1, ..., N$, then return to Step 2, setting $k = k + 1$.

8. Take $\{x_i^{m,(k)}\}$ as the final layer-adaptive mesh, $\{x_i^m\}$ for mth level and $Y_i^{m,(k)}$ as the required adaptive solution, Y_i^m at the mth time level.

9. Go to Step 1 with $m = m + 1$, repeat the same process for the adaptive mesh and solution at $(m + 1)$th time level.

The first test example is the following degenerate convection-diffusion singular perturbation problem [79].

Example 2.4.1.

$$\begin{cases} \varepsilon \frac{\partial^2 y}{\partial x^2}(x,t) + x^p \frac{\partial y}{\partial x}(x,t) - y(x,t) - \frac{\partial y}{\partial t}(x,t) = f(x,t), \quad (x,t) \in G, \\ y(x,t) = g(x,t), \quad (x,t) \in \partial G. \end{cases}$$

The functions f and g can be calculated from the exact solution

$$y(x,t) = e^{-t}\left(1 - x + xe^{-1/\sqrt{\varepsilon}} - e^{-x/\sqrt{\varepsilon}}\right).$$

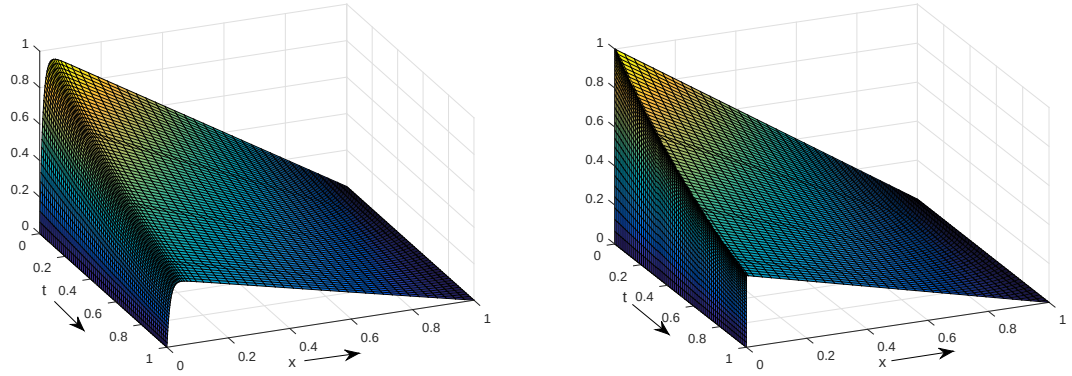

(a) $\varepsilon = 10^{-4}$ (b) $\varepsilon = 10^{-8}$

FIGURE 2.1: Surface plots of the numerical solution of Example 2.4.1 with $N = 64$, $p = 2$, $\varepsilon = 10^{-4}$, and $\varepsilon = 10^{-8}$.

Fig. 2.1 displays the surface plots for $\varepsilon = 10^{-4}$ and $\varepsilon = 10^{-8}$ with $N = 64$ and $p = 2$. From this figure one can clearly observe a boundary layer near Γ_l. For different values of M, N, and ε, we calculate the pointwise errors using the formula

$$E_{i,m}^{\varepsilon,N,M} = |Y_i^m - y(x_i^m, t_m)|.$$

We then calculate the maximum pointwise errors and the numerical rates of convergence by

$$E^{\varepsilon,N,M} = \max_{i,m} E^{\varepsilon,N,M}_{i,m}, \qquad F^{\varepsilon,N,M} = \log_2\left(\frac{E^{\varepsilon,N,M}}{E^{\varepsilon,2N,2M}}\right).$$

Finally, the parameter-robust errors and the parameter-robust rates of convergence are computed by

$$E^{N,M} = \max_{\varepsilon} E^{\varepsilon,N,M}, \qquad F^{N,M} = \log_2\left(\frac{E^{N,M}}{E^{2N,2M}}\right).$$

In Table 2.1, we display the errors $E^{\varepsilon,N,M}$ and $E^{N,M}$, and convergence rates $F^{\varepsilon,N,M}$

TABLE 2.1: Maximum pointwise errors $E^{\varepsilon,N,M}$, parameter-robust errors $E^{N,M}$, rates of convergence $F^{\varepsilon,N,M}$ and parameter-robust convergence $F^{N,M}$ using scheme (2.14) for Example 2.4.1 with $p = 2$.

ε	$N = 32$	$N = 64$	$N = 128$	$N = 256$	$N = 512$	$N = 1024$
10^{-1}	1.1134e-03	5.9091e-04	3.0455e-04	1.5456e-04	7.7859e-05	3.9075e-05
	0.9140	0.9563	0.9785	0.9892	0.9946	
10^{-2}	1.6582e-03	7.9905e-04	3.9089e-04	1.9331e-04	9.6134e-05	4.7937e-05
	1.0532	1.0325	1.0167	1.0088	1.0049	
10^{-3}	3.8783e-03	1.9834e-03	1.0077e-03	5.0730e-04	2.5449e-04	1.2724e-04
	0.9674	0.9769	0.9902	0.9952	1.0000	
10^{-4}	4.8593e-03	2.4942e-03	1.2707e-03	6.4184e-04	3.2171e-04	1.6086e-04
	0.9622	0.9730	0.9854	0.9965	0.9999	
10^{-5}	5.2579e-03	2.6824e-03	1.3657e-03	6.8888e-04	3.4636e-04	1.7313e-04
	0.9709	0.9739	0.9873	0.9919	1.0001	
10^{-6}	5.4821e-03	2.7604e-03	1.4010e-03	7.0610e-04	3.5560e-04	1.7758e-04
	0.9899	0.9784	0.9885	0.9896	1.0011	
10^{-7}	5.5818e-03	2.7898e-03	1.4162e-03	7.1248e-04	3.5910e-04	1.7918e-04
	0.9946	0.9781	0.9912	0.9885	1.0031	
10^{-8}	5.5840e-03	2.7974e-03	1.4199e-03	7.1554e-04	3.6051e-04	1.7975e-04
	0.9946	0.9782	0.9887	0.9889	1.0031	
$E^{N,M}$	5.5840e-03	2.7974e-03	1.4199e-03	7.1554e-04	3.6051e-04	1.7975e-04
$F^{N,M}$	0.9946	0.9782	0.9887	0.9889	1.0031	

and $F^{N,M}$. Here, we see that the error is decreasing as the number of mesh points are

increasing. From this table one can conclude that the proposed method is parameter-robust and the numerical results are completely in accordance with the theoretical result.

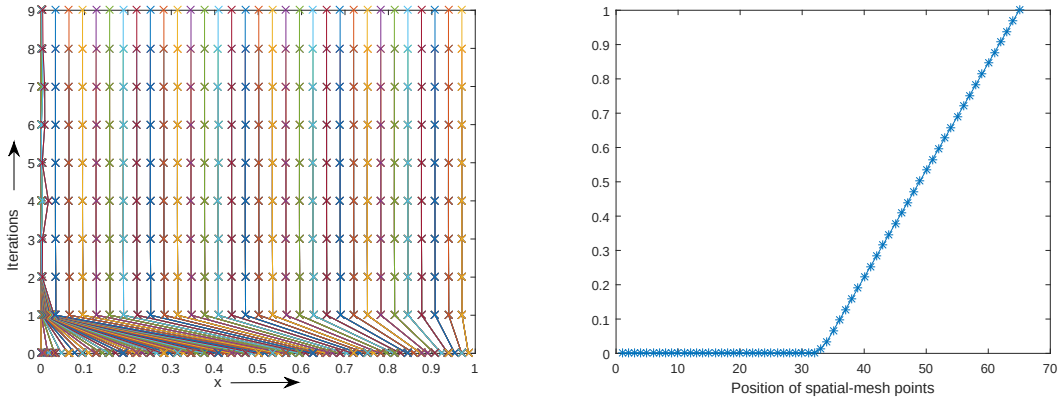

(a) Mesh trajectory (b) Position of space mesh points

FIGURE 2.2: Mesh trajectory and position of space mesh points taking $\varepsilon = 10^{-8}$, $N = 64$, and $p = 2$ at $t = 1$ for Example 2.4.1.

In Figure 2.2, we plot the movement of mesh points towards the boundary layer in each iteration of the mesh generation process and the final position of mesh points condensed in the layer region. This figure confirms the adaptive behavior of the mesh obtained through the equidistribution of our chosen monitor function.

The second test example is the following degenerate convection-diffusion singular perturbation problem [110].

Example 2.4.2.

$$\begin{cases} \varepsilon \frac{\partial^2 y}{\partial x^2}(x,t) + x^p \frac{\partial y}{\partial x}(x,t) - y(x,t) - \frac{\partial y}{\partial t}(x,t) = x^2 - 1, \quad (x,t) \in G, \\ y(x,0) = (1-x)^2, \quad x \in \bar{G}_x, \\ y(0,t) = 1 + t^2, \ y(1,t) = 0, \ t \in (0,T]. \end{cases}$$

Fig. 2.3 displays the surface plot for $\varepsilon = 10^{-2}$ and $\varepsilon = 10^{-5}$ with $N = 64$ and $p = 2$, from which a boundary layer can be clearly observed near Γ_l. The exact solution of

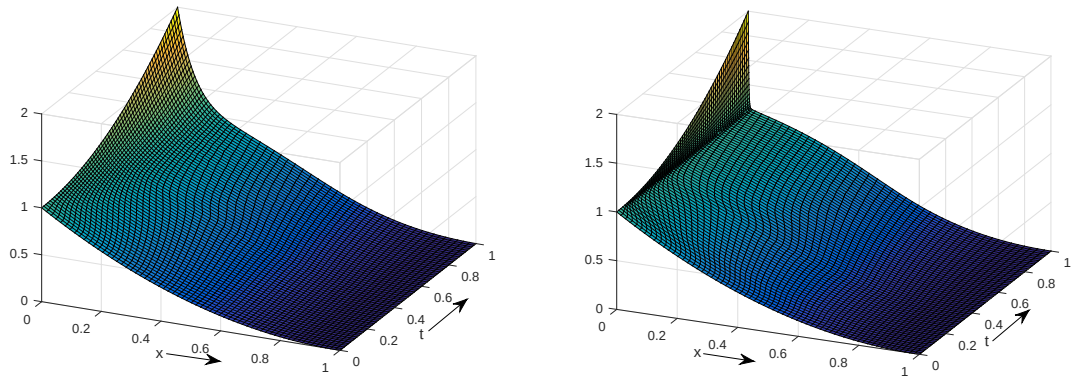

(a) $\varepsilon = 10^{-2}$ b $\varepsilon = 10^{-5}$

FIGURE 2.3: Surface plots of the numerical solution of Example 2.4.2 with $N = 64$, $p = 2$, $\varepsilon = 10^{-2}$ and $\varepsilon = 10^{-5}$.

Example 2.4.2 is not known, so to estimate numerical errors and rates of convergence we shall use the double mesh principle [6]. For this we bisect the spatial mesh and the time mesh, and then calculate the pointwise errors using the formula

$$E_{i,m}^{\varepsilon,N,M} = |Y_i^{m,2N,2M} - Y_i^{m,N,M}|.$$

Then the maximum pointwise errors and the rates of convergence are calculated by

$$E^{\varepsilon,N,M} = \max_{i,m} E_{i,m}^{\varepsilon,N,M}, \qquad F^{\varepsilon,N,M} = \log_2 \left(\frac{E^{\varepsilon,N,M}}{E^{\varepsilon,2N,2M}} \right).$$

Finally, the parameter-robust errors and parameter-robust rates of convergence are obtained by

$$E^{N,M} = \max_{\varepsilon} E^{\varepsilon,N,M}, \qquad F^{N,M} = \log_2 \left(\frac{E^{N,M}}{E^{2N,2M}} \right).$$

In Table 2.2, we present the results for Example 2.4.2. This table displays the errors $E^{\varepsilon,N,M}$ and $E^{N,M}$, and the convergence rates $F^{\varepsilon,N,M}$ and $F^{N,M}$. From these numerical results, again we observe that the method is first order parameter-robust for the addressed problem (2.1).

TABLE 2.2: Maximum pointwise errors $E^{\varepsilon,N,M}$, parameter-robust errors $E^{N,M}$, rates of convergence $F^{\varepsilon,N,M}$ and parameter-robust convergence $F^{N,M}$ using scheme (2.14) for Example 2.4.2 with $p = 1$.

ε	$N = 32$	$N = 64$	$N = 128$	$N = 256$	$N = 512$	$N = 1024$
10^{-1}	6.0678e-03	3.1060e-03	1.5716e-03	7.9055e-04	3.9646e-04	1.9852e-04
	0.9661	0.9828	0.9913	0.9957	0.99786	
10^{-2}	9.1940e-03	4.8423e-03	2.4863e-03	1.2594e-03	6.3381e-04	3.1793e-04
	0.92501	0.9617	0.9812	0.9906	0.9953	
10^{-3}	1.1452e-02	6.2810e-03	3.2832e-03	1.6747e-03	8.4525e-04	4.2453e-04
	0.9669	0.9356	0.9711	0.98650	0.9935	
10^{-4}	1.4429e-02	7.8765e-03	4.1433e-03	2.1086e-03	1.0578e-03	5.2844e-04
	0.8734	0.9268	0.9745	0.9951	1.0013	
10^{-5}	1.8039e-02	9.3421e-03	4.9472e-03	2.5223e-03	1.2580e-03	6.2199e-04
	0.9493	0.9172	0.9718	1.0035	1.0161	
10^{-6}	2.2009e-02	1.0476e-02	5.5412e-03	2.8546e-03	1.4341e-03	7.0988e-04
	1.0710	0.9188	0.9569	0.9931	1.0145	
10^{-7}	2.5967e-02	1.1221e-02	5.8996e-03	3.0621e-03	1.5543e-03	7.7683e-04
	1.2104	0.9275	0.9461	0.9783	1.0001	
10^{-8}	2.9611e-02	1.1848e-02	6.1079e-03	3.1723e-03	1.6194e-03	8.1577e-04
	1.3215	0.9359	0.9451	0.9701	0.98923	
$E^{N,M}$	2.9611e-02	1.1848e-02	6.1079e-03	3.1723e-03	1.6194e-03	8.1577e-04
$F^{N,M}$	1.3215	0.9359	0.9451	0.9701	0.98923	

In Figure 2.4, we provide log-log plots between the maximum pointwise errors and the number of spatial mesh points N, for both the test examples. From the slopes of these plots we can also validate first order convergence of the method. In Table 2.3, we present the results for different values of ϱ for Example 2.4.1 taking $\varepsilon = 10^{-7}$. This table displays the maximum pointwise errors $E^{\varepsilon,N,M}$, convergence rates $F^{\varepsilon,N,M}$, and the maximum number of iterations K required (over all time levels) before the stopping criterion in Step 6 of the algorithm is satisfied. From this table, we observe that values of ϱ close to 1 give slightly more accurate solutions but require more number of iterations. Further, we observe that the algorithm requires few iterations to converge.

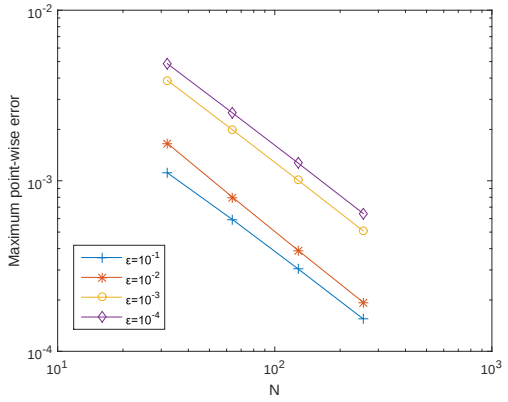

(a) Log-log plot for Example 2.4.1

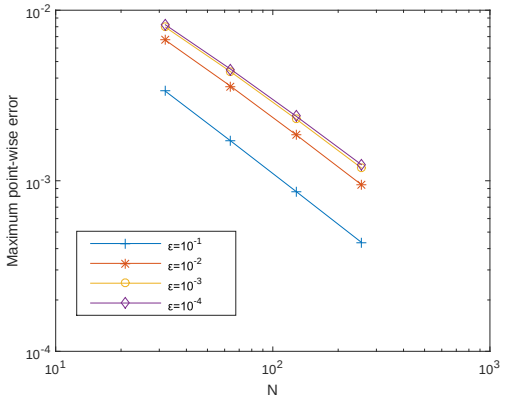

(a) Log-log plot for Example 2.4.2

FIGURE 2.4: Log-log plots of the maximum pointwise errors at time $t = 1$ for Examples 2.4.1 and 2.4.2.

TABLE 2.3: Maximum pointwise errors $E^{\varepsilon,N,M}$, rates of convergence $F^{\varepsilon,N,M}$, and the maximum number of iterations (over all time levels) K using different values of ϱ for Example 2.4.1 with $p = 2$ and $\varepsilon = 10^{-7}$.

ϱ		$N = 32$	$N = 64$	$N = 128$	$N = 256$	$N = 512$	$N = 1024$
$\varrho = 1.05$	$E^{\varepsilon,N,M}$	5.5818e-03	2.7898e-03	1.4162e-03	7.1248e-04	3.5910e-04	1.7918e-04
	$F^{\varepsilon,N,M}$	1.0005	0.9781	0.9912	0.9885	1.0029	
	K	12	7	7	6	5	4
$\varrho = 1.15$	$E^{\varepsilon,N,M}$	6.1339e-03	2.9877e-03	1.4609e-03	7.2179e-04	3.5916e-04	1.7919e-04
	$F^{\varepsilon,N,M}$	1.0378	1.0322	1.0172	1.0070	1.0031	
	K	10	6	5	5	4	3
$\varrho = 1.5$	$E^{\varepsilon,N,M}$	6.2798e-03	3.0429e-03	1.4616e-03	7.2169e-04	3.5900e-04	1.7919e-04
	$F^{\varepsilon,N,M}$	1.0453	1.0579	1.0181	1.0074	1.0025	
	K	6	5	4	4	3	3
$\varrho = 2.0$	$E^{\varepsilon,N,M}$	6.3449e-03	3.0370e-03	1.4616e-03	7.2079e-04	3.5900e-04	1.7919e-04
	$F^{\varepsilon,N,M}$	1.0629	1.0551	1.0199	1.0056	1.0025	
	K	4	4	4	3	3	3
$\varrho = 3.0$	$E^{\varepsilon,N,M}$	6.3449e-03	3.0370e-03	1.4616e-03	7.2079e-04	3.5900e-04	1.7919e-04
	$F^{\varepsilon,N,M}$	1.0629	1.0551	1.0199	1.0056	1.0025	
	K	4	4	4	3	3	3

2.5 Conclusions

We have proposed a numerical method comprising of the implicit Euler scheme on a uniform mesh in time direction and the upwind finite difference scheme on a layer-adaptive non-uniform mesh in spatial direction, for solving degenerate singularly

perturbed convection-diffusion problem. The layer-adaptive non-uniform mesh in spatial direction is generated through the equidistribution of the monitor function which is a combination of an appropriate power of second order derivative of the solution and a positive constant. It is shown through the truncation error and barrier function approach that the proposed method is parameter-robust with first order in both time and space. Numerical results are given for two test examples which validates the theoretical findings.

****